The Astrophysical Journal, 764:96 (7pp), 2013 February 10 doi:10.1088/0004-637X/764/1/96

CYG X-3: A GALACTIC DOUBLE BLACK HOLE OR BLACK-HOLE–NEUTRON-STAR PROGENITOR

Krzysztof Belczynski[1,2], Tomasz Bulik[1], Ilya Mandel[3], B. S. Sathyaprakash[4], Andrzej A. Zdziarski[5], and Joanna Mikołajewska[5]
[1] Astronomical Observatory, University of Warsaw, Al. Ujazdowskie 4, 00-478 Warsaw, Poland
[2] Center for Gravitational Wave Astronomy, University of Texas at Brownsville, Brownsville, TX 78520, USA
[3] School of Physics and Astronomy, University of Birmingham, Edgbaston B15 2TT, UK
[4] School of Physics and Astronomy, Cardiff University, 5, The Parade, Cardiff CF24 3YB, UK
[5] Centrum Astronomiczne im. M. Kopernika, Bartycka 18, PL-00-716 Warszawa, Poland
Received 2012 September 12; accepted 2012 December 19; published 2013 January 29

ABSTRACT

There are no known stellar-origin double black hole (BH–BH) or black-hole–neutron-star (BH–NS) systems. We argue that Cyg X-3 is a very likely BH–BH or BH-NS progenitor. This Galactic X-ray binary consists of a compact object, wind-fed by a Wolf-Rayet (W-R) type companion. Based on a comprehensive analysis of observational data, it was recently argued that Cyg X-3 harbors a 2–4.5 $M_\odot$ black hole (BH) and a 7.5–14.2 $M_\odot$ W-R companion. We find that the fate of such a binary leads to the prompt ($\lesssim$1 Myr) formation of a close BH–BH system for the high end of the allowed W-R mass ($M_{\rm W\text{-}R} \gtrsim 13\,M_\odot$). For the low- to mid-mass range of the W-R star ($M_{\rm W\text{-}R} \sim 7$–$10\,M_\odot$) Cyg X-3 is most likely (probability 70%) disrupted when W-R ends up as a supernova. However, with smaller probability, it may form a wide (15%) or a close (15%) BH–NS system. The advanced LIGO/VIRGO detection rate for mergers of BH–BH systems from the Cyg X-3 formation channel is $\sim$10 yr^{-1}, while it drops down to $\sim$0.1 yr^{-1} for BH–NS systems. If Cyg X-3 *in fact* hosts a low-mass black hole and massive W-R star, it lends additional support for the existence of BH–BH/BH–NS systems.

Key words: binaries: general – stars: neutron – X-rays: binaries

Online-only material: color figures

1. INTRODUCTION

Ever since the discovery of the Hulse–Taylor pulsar PSR B1913+16 (Weisberg & Taylor 2005), a system consisting of a pair of neutron stars, there has been a lot of effort to detect other double compact objects with neutron stars and black holes. So far only double neutron star (NS–NS) systems have been found (e.g., Lorimer 2008). In particular, no black-hole-neutron-star (BH–NS) or stellar-mass double black hole (BH–BH) systems are known at the moment.

Merging compact binaries have provided the strongest motivation yet to build wide-band interferometric gravitational wave detectors. Second-generation detectors, the Laser Interferometer Gravitational-wave Observatory (LIGO) in the U.S. (Harry 2010), Virgo in Italy (Acernese et al. 2006), and KAGRA[6] in Japan, have the potential to observe the late inspiral and merger phases of compact binaries with total mass in the range $\sim[1,\ 10^3]\,M_\odot$. The range of masses they could observe is determined by the frequency window of $\sim[10,\ 10^4]$ Hz in which they operate. Observed Galactic radio binary pulsars lend strong motivation for the existence of merging systems at the lower end of the above mass range. When LIGO, Virgo, and KAGRA begin their observations later in this decade, they could well provide the observational evidence for heavier BH–NS/BH–BH systems and set very strong constraints on the statistics of their populations. However, we now have a plausible progenitor of a BH–NS/BH–BH system in our own Galaxy.

High-mass X-ray binaries (HMXBs) provide a unique opportunity to study various astrophysical phenomena. At *Warsaw Observatory* we have undertaken a program to study HMXBs in the context of the formation of double compact objects like BH–BH or BH–NS systems. We have already provided studies of two extragalactic HMXBs that host the most massive known BHs of stellar origin: IC 10 X-1 and NGC 300 X-1 (Bulik et al. 2011), an analysis of the Cyg X-1 binary that harbors the most massive stellar black hole (BH) in our Galaxy (Belczynski et al. 2011), and analyses of several other binaries with well-established parameters: GX 301−2, Vela X-1, XTE J1855−026, 4U 1907+09, Cir X-1, LMC X-1, LMC X-3, and M33 X-1 (Belczynski et al. 2012a).

In this study, we follow the recent estimate of system parameters for another Galactic HMXB: Cyg X-3. Zdziarski et al. (2012) have estimated that Cyg X-3 consists of a low-mass BH, 2–4.5 $M_\odot$, and a massive Wolf-Rayet (W-R) star, 7.5–14.2 $M_\odot$. We use this estimate to calculate the future evolution of Cyg X-3 to check whether this binary may provide any observational constraints on as-yet undetected BH–BH and BH–NS systems. The past evolution of Cyg X-3 was studied in detail by Lommen et al. (2005).

2. ESTIMATES

2.1. The Future Evolution of Cyg X-3

Future evolution of Cyg X-3 has been considered in the past only qualitatively, by Ergma & Yungelson (1998) and Lommen et al. (2005). Ergma & Yungelson (1998) assumed that the present W-R star mass is $M_{\rm W\text{-}R} = 10\,M_\odot$, and they estimated W-R lifetime to be 5×10^5 yr. They also calculated that the period will change from the current value of $P_{\rm orb} = 4.8$ hr to $P_{\rm orb} \simeq 8$ hr at the time of core collapse/supernova (SN). At this point they estimated that W-R star mass will decrease to $M_{\rm W\text{-}R} \simeq 5\,M_\odot$. If this W-R star collapses into a BH, it will merge with the other BH after 4×10^8 yr. If instead a neutron star (NS) is formed, they find that the system will not merge in

[6] http://www.icrr.u-tokyo.ac.jp/gr/LCGT.html

the Hubble time. For the BH case, findings of Lommen et al. (2005) are similar to those of Ergma & Yungelson (1998).

Here, we describe in detail Cyg X-3 evolutionary scenarios leading to the formation of a BH–BH or BH–NS system. For demonstration we choose extremes of the allowed mass range of BH and W-R components: $M_{\rm BH1} = 2.0\,M_\odot$ with $M_{\rm W\text{-}R} = 7.5\,M_\odot$ and $M_{\rm BH1} = 4.5\,M_\odot$ with $M_{\rm W\text{-}R} = 14.2\,M_\odot$. Additionally, we evolve the most likely configuration $M_{\rm BH1} = 2.4\,M_\odot$ with $M_{\rm W\text{-}R} = 10.3\,M_\odot$ adopted from Zdziarski et al. (2012). First, we employ our standard model for stellar and binary evolution (see below), and in the next section we will test how various evolutionary uncertainties change our results.

We evolve three $M_{\rm zams} = 27, 36, 50\,M_\odot$ single stars (Hurley et al. 2000) at solar metallicity $Z = 0.02$ with our calibrated wind mass-loss rates (Belczynski et al. 2010a). At $t = 6.5, 5.2, 4.4$ Myr these stars leave the main sequence (MS) and become Hertzsprung gap objects with helium core of $M_{\rm W\text{-}R,i} = 7.5, 10.3, 14.2\,M_\odot$, respectively. We expose[7] this core right after MS and make them naked helium stars: massive W-R objects. We pair these W-R stars with $M_{\rm BH1} = 2.0, 2.4, 4.5\,M_\odot$ BHs and create three binaries all with the orbital period of $P_{\rm orb} = 4.8$ hr, as observed for Cyg X-3. Such an approach allows a W-R star to shed the maximum amount of mass, reducing its chance to become NS or BH, and thus makes our estimates conservative. In other words, we allow for the maximum lifetime of a W-R star and as a consequence (due to mass loss) obtain a lower mass limit on the W-R star mass (within our evolutionary model) at the time of core collapse. This leads to the lower limit on the compact object mass (whether it is an NS or a BH) formed in the core collapse/supernova event. This in turn results in the lower limits of LIGO/VIRGO detection rates as these increase with compact object mass (see Section 2.3).

Stars in isolation may evolve differently than stars in binary systems. The major factor that influences the evolution of a star in a binary system (besides mass transfer episodes) is tidal interactions that affect the rotation of a given star. For low- and intermediate-mass stars, tides are efficient enough that the evolution of a given star may be affected via increased rotation (e.g., increased convection, mixing of elements, overshooting). For example, this scenario is discussed in detail by Podsiadlowski et al. (2004) for the case of intermediate-mass progenitors of neutron stars. For massive stars, the tidal interactions are very inefficient (radiative damping) as indicated by stellar models presented by Claret (2007). Massive stars in close binaries do not significantly change their rotation by the time they reach Roche lobe overflow. In the case of Cyg X-3, the W-R star is rather massive, indicating a very massive progenitor star: ∼30–50 $M_\odot$. Evolution of such a star is not greatly affected by tidal interactions with a rather light (∼2–5 $M_\odot$) companion in terms of rotation, mixing, and internal evolution. The primary evolutionary influence of the companion is the removal of the H-rich envelope that forms a close binary and exposes the W-R star itself.

The binary separations at the currently observed orbital period of the three synthetic binaries are $a = 3.0, 3.4, 3.8\,R_\odot$, and the Roche lobe radii of the W-R component are $R_{\rm lobe} = 1.5, 1.7, 1.8\,R_\odot$. The corresponding radii of W-R stars are $R_{\rm W\text{-}R} = 0.8, 1.0, 1.2\,R_\odot$. Massive helium stars do not expand at any significant level during evolution. For example, the largest expansion is expected for the lowest mass model ($M_{\rm W\text{-}R} = 7.4\,M_\odot$), and this star can reach $R_{\rm W\text{-}R} = 1.6\,R_\odot$. This happens late in its evolution, and by this time the orbit has expanded and the corresponding Roche lobe radius is $R_{\rm lobe} = 1.8\,R_\odot$. For more massive W-R stars ($M_{\rm W\text{-}R} > 10\,M_\odot$), there is virtually (within 10%) no radial expansion (e.g., Hurley et al. 2000). Therefore, no Roche lobe mass transfer episode is expected in the future evolution of these systems.

The lifetimes of these W-R stars are $t_{\rm W\text{-}R} = 0.95, 0.77, 0.64$ Myr, and at the end of their evolution the masses drop to $M_{\rm W\text{-}R,f} = 5.5, 6.8, 8.2\,M_\odot$. We use the wind mass-loss rate based on Hurley et al. (2000), which takes into account effects of clumping (Hamann & Koesterke 1998),

$$(dM/dt) = 10^{-13}\left(\frac{L}{L_\odot}\right)^{1.5} M_\odot\ {\rm yr}^{-1}. \quad (1)$$

This prescription is based on detailed stellar evolutionary calculations combined with comprehensive W-R wind models and calibrated on observations of three W-R stars. We then obtain W-R star luminosity, $L(M_{\rm W\text{-}R})$, from evolutionary models of Hurley et al. (2000).

At the time of explosion, the orbits have expanded to $a = 3.9, 4.7, 5.6\,R_\odot$ due to the W-R wind mass-loss and W-R stars have formed massive CO cores ($M_{\rm CO} = 4.0, 5.0, 6.2\,M_\odot$). The W-R stars undergo a core collapse. We use the Fryer et al. (2012) rapid explosion model that reproduces the observed mass gap between neutron stars and black holes (Belczynski et al. 2012b). For the initial $M_{\rm W\text{-}R,i} = 7.5, 10.3\,M_\odot$, the core collapse is followed by Type Ib supernovae and neutron stars form with mass $M_{\rm NS} = 1.5, 1.7\,M_\odot$, respectively. The mass loss and natal kicks associated with supernovae are very likely to disrupt these two synthetic binaries (with the probability of $f_{\rm disruption} = 0.69$). However, there is also a significant chance to form a close BH–NS system. We estimate the probability of the BH–NS system formation with gravitational merger time $T_{\rm merger}$ shorter than 10 Gyr at the level $f_{\rm close} = 0.14, 0.12$ for the low- and intermediate-mass realization of Cyg X-3. We have applied a distribution of natal kicks as derived from the population of Galactic pulsars (Hobbs et al. 2005). The kicks have a random direction, and their magnitude is taken from a single Maxwellian with $\sigma = 265$ km s^{-1}. Additionally, we lower the magnitude of natal kicks due to the amount of fallback expected in each supernova explosion by factor $(1 - f_{\rm fb})$ (Fryer et al. 2012). The fallback amount, the fraction of matter that was initially ejected in a supernova explosion but that is later accreted back onto the compact object, was estimated to be $f_{\rm fb} = 0.14, 0.16$ in case of models with initial $M_{\rm W\text{-}R,i} = 7.5, 10.3\,M_\odot$, respectively.

For the high component-mass realization ($M_{\rm W\text{-}R,i} = 14.2\,M_\odot$) within our rapid supernova explosion model, the entire W-R star falls into a BH (i.e., $f_{\rm fb} = 1.0$). We assume the loss of 10% of the gravitational mass during the collapse through neutrino emission, which leads to a slight orbital expansion and a small induced eccentricity ($a = 6.0\,R_\odot$, $e = 0.07$). In the end, the second BH forms with mass $M_{\rm BH,2} = 7.4\,M_\odot$. No natal kick is imparted on a BH within this model. Therefore, a close BH–BH system forms with a chirp mass of $M_{\rm c,dco} \equiv (M_1 M_2)^{3/5}(M_1 + M_2)^{-1/5} = 5.0\,M_\odot$ and a merger time of $T_{\rm merger} = 0.5$ Gyr. In this particular case with no natal kick, there is no other possibility ($f_{\rm close} = 1.0$), within the framework of our model, but to form a close ($T_{\rm merger} < 10$ Gyr) BH–BH system.

If we conservatively assume that at any given time there is only one such system as Cyg X-3, it means that the Galactic

[7] The H-rich envelope was removed artificially from a star in one very short evolutionary time step. The exposed core continues its evolution as a naked He star following evolutionary tracks calculated by O. Pols (Hurley et al. 2000).

Table 1
Fate of Cyg X-3

$M_{BH} + M_{W\text{-}R}$	Wind[a]/Kicks[b]/SN[c]	Outcome[d]	f_{close}[e]	$M_{c,dco}$	t_{W-R}	$\mathcal{R}_{MW}$	$\mathcal{R}_{GW}$
$2.0 + 7.5\ M_\odot$	Theory/low/rapid	BH–NS ($2.0 + 1.5\ M_\odot$)	0.18	$1.5\ M_\odot$	0.95 Myr	$0.19\ \mathrm{Myr}^{-1}$	$0.09\ \mathrm{yr}^{-1}$
$2.4 + 10.3\ M_\odot$	Theory/low/rapid	BH–NS ($2.4 + 1.7\ M_\odot$)	0.15	$1.8\ M_\odot$	0.77 Myr	$0.20\ \mathrm{Myr}^{-1}$	$0.13\ \mathrm{yr}^{-1}$
$4.5 + 14.2\ M_\odot$	Theory/low/rapid	BH–BH ($4.5 + 7.4\ M_\odot$)	1.00	$5.0\ M_\odot$	0.64 Myr	$1.56\ \mathrm{Myr}^{-1}$	$11.3\ \mathrm{yr}^{-1}$
$2.0 + 7.5\ M_\odot$	Empiri/low/rapid	BH–NS ($2.0 + 1.5\ M_\odot$)	0.18	$1.5\ M_\odot$	0.95 Myr	$0.19\ \mathrm{Myr}^{-1}$	$0.09\ \mathrm{yr}^{-1}$
$2.4 + 10.3\ M_\odot$	Empiri/low/rapid	BH–NS ($2.4 + 1.8\ M_\odot$)	0.15	$1.8\ M_\odot$	0.76 Myr	$0.20\ \mathrm{Myr}^{-1}$	$0.14\ \mathrm{yr}^{-1}$
$4.5 + 14.2\ M_\odot$	Empiri/low/rapid	BH–BH ($4.5 + 8.0\ M_\odot$)	1.00	$5.2\ M_\odot$	0.64 Myr	$1.57\ \mathrm{Myr}^{-1}$	$12.4\ \mathrm{yr}^{-1}$
$2.0 + 7.5\ M_\odot$	Theory/high/rapid	BH–NS ($2.0 + 1.5\ M_\odot$)	0.19	$1.5\ M_\odot$	0.95 Myr	$0.20\ \mathrm{Myr}^{-1}$	$0.09\ \mathrm{yr}^{-1}$
$2.4 + 10.3\ M_\odot$	Theory/high/rapid	BH–NS ($2.4 + 1.7\ M_\odot$)	0.17	$1.8\ M_\odot$	0.77 Myr	$0.22\ \mathrm{Myr}^{-1}$	$0.15\ \mathrm{yr}^{-1}$
$4.5 + 14.2\ M_\odot$	Theory/high/rapid	BH–BH ($4.5 + 7.4\ M_\odot$)	0.68	$5.0\ M_\odot$	0.64 Myr	$1.06\ \mathrm{Myr}^{-1}$	$7.7\ \mathrm{yr}^{-1}$
$2.0 + 7.5\ M_\odot$	Theory/low/delayed	BH–NS ($2.0 + 1.9\ M_\odot$)	0.26	$1.7\ M_\odot$	0.95 Myr	$0.27\ \mathrm{Myr}^{-1}$	$0.17\ \mathrm{yr}^{-1}$
$2.4 + 10.3\ M_\odot$	Theory/low/delayed	BH–BH ($2.4 + 2.7\ M_\odot$)	0.28	$2.2\ M_\odot$	0.77 Myr	$0.36\ \mathrm{Myr}^{-1}$	$0.41\ \mathrm{yr}^{-1}$
$4.5 + 14.2\ M_\odot$	Theory/low/delayed	BH–BH ($4.5 + 3.9\ M_\odot$)	0.50	$3.6\ M_\odot$	0.64 Myr	$0.78\ \mathrm{Myr}^{-1}$	$2.8\ \mathrm{yr}^{-1}$

Notes.
[a] Either theoretically (Equation (1)) or empirically (Equation (3)) based W-R wind mass-loss rates are applied.
[b] High: NS and BH kicks are taken from a Maxwellian with $\sigma = 265$ km s^{-1}. Low: the high kicks are decreased proportionally to the amount of fallback for both NSs and BHs.
[c] Compact-object formation model: via either rapid supernovae (mass gap) or delayed supernovae (no mass gap).
[d] Type of binary formed followed by the mass of compact objects.
[e] We only count binaries that have formed with merger time shorter than 10 Gyr (others are disrupted or form wider systems).

birthrate is at the level $\mathcal{R}_{birth} = 1/t_{W\text{-}R}$. As listed above, lifetimes of the considered massive W-R stars are very short, $t_{W\text{-}R} \lesssim 1$ Myr. Since the merger times of systems that we include in our analysis are relatively short ($T_{merger} < 10$ Gyr) and the star formation was approximately constant in the Galactic disk over a long period of time (∼10 Gyr), the Galactic merger rate of BH–NS and BH–BH systems may be estimated from

$$\mathcal{R}_{MW} = f_{close}\mathcal{R}_{birth} \sim \frac{f_{close}}{t_{W\text{-}R}}. \quad (2)$$

We discuss statistical uncertainties in the estimate of the birthrates in Section 2.4. For our three Cyg X-3 realizations, we obtain $\mathcal{R}_{MW} = 0.19, 0.20\ \mathrm{Myr}^{-1}$ in the cases of BH–NS formation and $\mathcal{R}_{MW} = 1.56\ \mathrm{Myr}^{-1}$ in the case of BH–BH formation. The main results presented in this section are summarized in Table 1 (top three entries) and illustrated in Figure 1 (top panel).

2.2. Range of Evolutionary Uncertainties

Alternatively to our standard approach, we employ W-R wind mass-loss rates adopted from Zdziarski et al. (2012):

$$(dM/dt) = 1.9 \times 10^{-5} \left(\frac{M_{W\text{-}R}}{14.7\ M_\odot}\right)^{2.93} M_\odot\ \mathrm{yr}^{-1}. \quad (3)$$

Zdziarski et al. (2012) selected data points from Nugis & Lamers (2000) for W-R stars of similar mass and type as the one in Cyg X-3. Nugis & Lamers (2000) have estimated clumping-corrected mass-loss rates based on observations and modeling of 64 Galactic W-R stars. We refer to this wind mass-loss prescription as empirical as it is heavily derived from observations in contrast to the method used in our standard approach (mostly originating from theoretical predictions). In particular, Zdziarski et al. (2012) employed data points from Table 5 of Nugis & Lamers (2000) for W-R stars. It is worth noting that the majority of these W-R stars (19 out of 34) are in binary systems. The results of calculations with those winds are presented in Table 1 (models marked with "Wind: empiri") and in Figure 1 (bottom panel). It is noted that both wind mass-loss prescriptions give very similar results. There is no significant change in our analysis. There is only a slight increase of BH mass ($M_{BH,2} = 8.0\ M_\odot$) in the case of BH–BH formation.

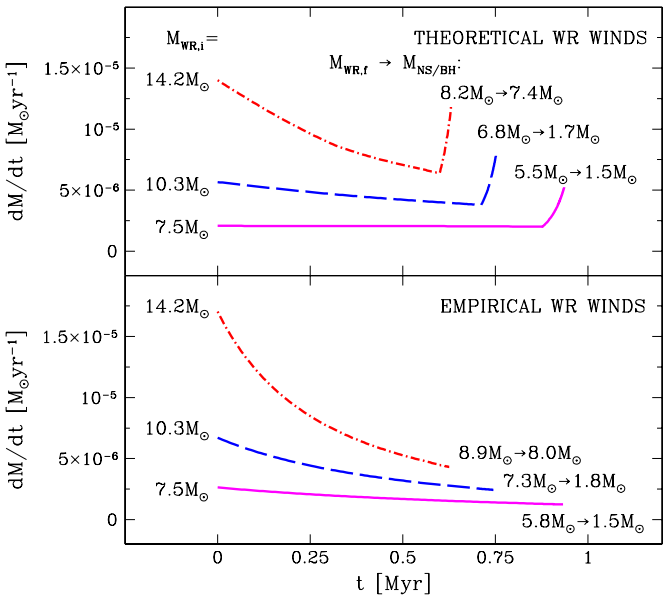

Figure 1. Evolutionary prediction for Cyg X-3 W-R star ($M_{W\text{-}R,i} = 10.3^{+3.9}_{-2.8}\ M_\odot$). The top panel shows the wind mass-loss rate based on theoretical calculations, while results in the bottom panel are based on observationally estimated W-R mass-loss rates. The upturns of dM/dt in the top panel are due to shell burning at the end of the evolution. Independent of the adopted wind mass-loss rate, the W-R component becomes either a neutron star for low- to medium-mass progenitors ($M_{W\text{-}R,i} = 7.5$–$10.3\ M_\odot$) or a black hole at the high end ($M_{W\text{-}R,i} = 14.2\ M_\odot$) of the allowed W-R mass range. The mass of the W-R component at the end of its evolution is marked with $M_{W\text{-}R,f}$, while the mass of the compact object formed after core collapse/supernova explosion is marked with $M_{NS/BH}$. Compact objects with $M_{NS/BH} < 2\ M_\odot$ are assumed to be neutron stars, and above that, black holes.

(A color version of this figure is available in the online journal.)

Next, we alternate our approach to natal kicks. We adopt high kicks for all compact objects. It means that both neutron stars and black holes receive kicks from the same distribution described by a Maxwellian with $\sigma = 265$ km s^{-1}. There is no kick

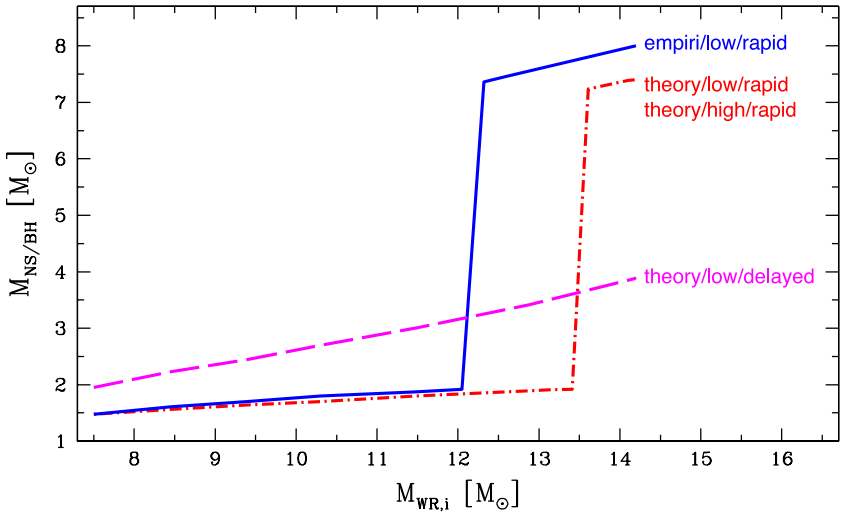

Figure 2. Dependence of the second compact object mass on the current W-R star mass for Cyg X-3. There is a sharp transition from NS to BH formation for the rapid SN engine at around $M_{\rm W\text{-}R,i} \sim 12$–$13\,M_\odot$. The delayed SN engine allows for a steady increase of compact-object mass, and the NS/BH transition depends sensitively on the unknown maximum NS mass. The assumed kick velocity has no impact on the compact-object mass, so two kick models (theory/low/rapid and theory/high/rapid) yield the same mass spectrum for the second compact object.

(A color version of this figure is available in the online journal.)

decrease factor applied in this case. Results for such an approach are listed in Table 1 (marked with "Kicks: high"). There is no significant change for the BH–NS formation, as neutron stars in our standard model analysis were receiving almost full kicks (low fallback). There is a noticeable decrease in the formation efficiency of close BH–BH systems ($f_{\rm close} = 0.68$) that leads to a corresponding decrease in the Galactic merger rate ($\mathcal{R}_{\rm MW} = 1.06\ {\rm Myr}^{-1}$). The decrease is caused by binary disruptions due to high natal kicks applied to black holes in this model. However, the formation efficiency is still significant despite the rather high kicks that black holes receive in this model, because the binary's orbital velocity at core collapse, $\sim$800 km s^{-1}, is already large compared with typical kicks.

Our calculations so far were based on the rapid supernova explosion engine, in which a sufficiently massive progenitor does not explode at all, gets no natal kick, and forms quite a massive black hole. In the rapid model this is the reason for the emergence of a mass gap between NS and BH masses (Belczynski et al. 2012b, although see Kreidberg et al. 2012). On the one hand, lower mass stars are subject to strong explosions and form neutron stars (as in the case of $M_{\rm W\text{-}R} = 7.5, 10.3\,M_\odot$). On the other hand, higher mass stars do not explode at all and form massive black holes (as for $M_{\rm W\text{-}R} = 14.2\,M_\odot$). This explains the rather sharp transition for all models considered thus far from $M_{\rm W\text{-}R} = 10.3\,M_\odot$ forming a neutron star ($M_{\rm NS} = 1.7$–$1.8\,M_\odot$) to $M_{\rm W\text{-}R} = 14.2\,M_\odot$ forming quite a massive black hole ($M_{\rm BH2} = 7.4$–$8\,M_\odot$).

As a final variant, we have modified our approach to supernova explosions. We now use the delayed explosion model of Fryer et al. (2012). This model generates a continuous compact-object mass spectrum (i.e., without a mass gap). The results for this set of calculations are listed in Table 1 (marked with "SN: delayed"). Due to the delayed nature of the explosion engine, neutron stars are typically more massive as proto-neutron stars have more time for accretion between the core bounce and actual explosion. The explosions are also typically less energetic, since at later times, after some cooling, there is less energy to drive the explosion. This leads to two changes for BH–NS formation. First, there is a noticeable increase in the formation efficiency (lower explosion energy leads to increased fallback and smaller natal kicks). Second, we note a significant increase in the NS mass. In fact, for the most likely Cyg X-3 configuration ($M_{\rm BH1} = 2.4\,M_\odot$; $M_{\rm W\text{-}R} = 10.3\,M_\odot$), instead of forming an NS ($M_{\rm NS} = 1.7$–$1.8\,M_\odot$ in all other models), we obtain a low-mass black hole ($M_{\rm BH2} = 2.7\,M_\odot$) and thus transition from BH–NS to BH–BH formation. In the case of the Cyg X-3 high-mass configuration we predict as before the formation of a BH–BH binary. The black hole in this model is formed with moderate fallback ($f_{\rm fb} = 0.43$) and therefore receives a moderate natal kick. It has a significantly lower mass ($M_{\rm BH2} = 3.9\,M_\odot$), since the majority of the ejected material was not subject to fallback. As a result, the formation efficiency is noticeably smaller ($f_{\rm close} = 0.5$) relative to all other models. Figure 2 shows the mass of the final compact object as a function of the initial mass of the W-R star for all alternative models considered in this section.

If rotation is included for W-R stars (e.g., Georgy et al. 2012), the W-R core mass will increase. In such a case, it is expected that the compact object that forms out of a given W-R star may (possibly) be somewhat heavier as contrasted with our non-rotating models. We say "possibly" as the rotation also increases the mass-loss rate and may increase W-R lifetime; both of these effects may slightly decrease the mass of the compact object. If indeed the mass of the compact object increases with rotation, it is possible that some of our $10.3\,M_\odot$ W-R star models would form a BH instead of an NS and the detection chances would slightly increase. To quantify this change, we may compare the model that produces $2.4 + 1.7\,M_\odot$ BH–NS (detection rate: 0.13 yr^{-1}) with $2.4+2.7\,M_\odot$ BH–BH (detection rate: 0.41 yr^{-1}). Although there may be some moderate quantitative changes, qualitatively our conclusions remain the same.

2.3. LIGO/VIRGO Detection Rate Estimate

In order to compute the advanced LIGO/Virgo event rates, we use the same detection threshold that was adopted in Abadie et al. (2010)—a signal-to-noise ratio (S/N) of 8 in a single interferometer at the sensitivity of advanced LIGO. This is a simplified treatment, since actual detector sensitivity will

depend on the network configuration, data quality, and the details of the search pipeline, but the uncertainties introduced by this simplifying assumption are smaller than the evolutionary uncertainties in the merger rates.

Previous calculations in the population-synthesis literature (e.g., Belczynski et al. 2010b) were based on a simple scaling of the detection volume for arbitrary systems with the horizon distance d_0 for an NS–NS binary (the distance at which an optimally oriented source with component masses $M_1 = M_2 = 1.4\,M_\odot$ could be detected at an S/N of 8):

$$\mathcal{R}_{\rm GW} = \rho_{\rm gal}\frac{4\pi}{3}\left(\frac{d_0}{f_{\rm pos}}\right)^3\left(\frac{\mathcal{M}_{\rm c,dco}}{\mathcal{M}_{\rm c,nsns}}\right)^{15/6}\mathcal{R}_{\rm MW}. \quad (4)$$

Here $\rho_{\rm gal}$ is the density of Milky-Way-like galaxies, the chirp mass $\mathcal{M}_{\rm c,nsns} \equiv M_1^{3/5}M_2^{3/5}(M_1+M_2)^{-1/5} = 1.2\,M_\odot$, and the correction factor $f_{\rm pos} = 2.26$ takes into account the non-uniform pattern of detector sensitivity and random sky location and orientation of sources (Finn 1996).

However, this simple calculation suffered from several shortcomings. The sensitivity distance scales as $d \sim d_0(\mathcal{M}_{\rm c,dco}/\mathcal{M}_{\rm c,nsns})^{5/6}$ only for masses sufficiently low that the gravitational-wave signal spans the bandwidth of the detector. The waveforms used to compute the horizon distance included only the contribution from the inspiral portion, not the merger and ringdown signals. Finally, cosmological effects due to the expansion of the universe have not been included: the redshifting of the gravitational waveform itself, which can be described by the dilation of masses, the difference between the volume as a function of luminosity distance d and comoving volume, and the difference in the rate of clocks in the source and merger frames. Here we include these effects by using the following procedure when integrating over shells centered on the detector:

1. For each shell at a given redshift z, compute the luminosity distance $d(z)$ and the comoving volume of the shell $dV_c(z)$ using standard cosmology (see, e.g., Hogg 1999) with $\Omega_M = 0.272$, $\Omega_\Lambda = 0.728$, $h = 70.4$ (WMAP 7 results).
2. Given a particular combination of compact-object masses from Table 1, compute the S/N for an optimally oriented source at distance $d(z)$,

$$\mathrm{S/N}^2 = 4\int_0^\infty \frac{|\tilde{h}(f_{\rm GW})|^2}{S_n(f_{\rm GW})}df_{\rm GW}, \quad (5)$$

   where we use the inspiral–merger–ringdown waveform family IMRPhenomB (Ajith et al. 2011) to compute the frequency-domain waveforms $\tilde{h}(f_{\rm GW})$ using redshifted component masses $M \rightarrow M(1+z)$ and the zero-detuning, high-power[8] Advanced LIGO noise power spectral density $S_n(f_{\rm GW})$ (Harry 2010).
3. Compute the fraction of detectable mergers $f_{\rm det}(z)$ from this shell by considering the fraction of sources for which the projection function $\Theta(\iota,\theta,\psi,\phi) \leqslant 4$ (given in Equations (3.4.b)– (3.4.d) of (Finn 1996)) is large enough so that $(\Theta/4)\mathrm{S/N} \geqslant 8$. The cumulative distribution function of Θ can be computed numerically (the approximate expression given by Finn (1996), not being sufficiently accurate) via a Monte Carlo over the inclination angle ι (whose cosine is uniform in [0, 1]), the sky-location spherical coordinates θ (whose cosine is uniform in [0, 1]) and ϕ (uniform in $[0, 2\pi]$), and polarization ψ (uniform in $[0, \pi]$).
4. The contribution of the shell to the detection rate is given by $f_{\rm det}(z)dV_c(z)\rho_{\rm gal}\mathcal{R}_{\rm MW}(1+z)^{-1}$. We assume that the intrinsic merger rate in the source frame is independent of redshift (i.e., we do not include the dependence of star formation rate or metallicity on redshift). Thus, we use $\mathcal{R}_{\rm MW}$ from Table 1 and scale it by the space density of Milky-Way-like galaxies, for which we use 0.01 Mpc^{-3} of comoving volume (Abadie et al. 2010). The final factor of $1/(1+z)$ reflects the time dilation between the source clock, used to measure the merger rate, and the clock on Earth, used to measure the detection rate.

We can now integrate over multiple shells (or, in practice, compute an approximate Riemann sum over the shells numerically) to obtain the advanced LIGO/Virgo detection rates that we report in Table 1. Including merger and ringdown waveform phases of the coalescence waveform yields more power than is available in the inspiral alone and thus tends to increase detection rates; this effect is greatest for high-mass systems: the correction would be negligible for NS–NS systems[9] and amounts to ∼15% for a BH–BH system with $10M_\odot$ components. The redshifting of the gravitational-wave signal can increase the power in the sensitive band of the detectors by a factor of up to $(1+z)^{5/6}$ for low-mass systems. However, cosmological corrections tend to decrease the detected event rate relative to the simple scaling of Equation (4), largely because the comoving volume within a luminosity distance d is significantly smaller than $(4/3)\pi d^3$ at non-trivial redshifts. Incorporating the full set of waveform and cosmological corrections as described above decreases predicted detection rates by $\gtrsim$15% for BH–NS systems and by $\gtrsim$30% for BH–BH systems relative to the simple scaling calculation.

2.4. Statistical Uncertainty on Merger and Detection Rates

We note that the rates derived above do not account for the statistical uncertainty associated with observing a single binary like Cyg X-3. In practice, we do not know the exact rate from a single observation even if $f_{\rm close}$ and $t_{\rm W-R}$ are known perfectly in Equation (2). Assuming that the birth of binaries like Cyg X-3 is a stochastic Poisson process with rate $\mathcal{R}_{\rm birth}$, the probability of electromagnetically observing exactly one such system is

$$p(1\ \mathrm{obs.}|\mathcal{R}_{\rm birth}) = \mathcal{R}_{\rm birth}\mathrm{t_{W\text{-}R}}\exp\left(-\mathcal{R}_{\rm birth}\mathrm{t_{W\text{-}R}}\right). \quad (6)$$

We can compute the probability distribution on the rate given a single observation by using Bayes' theorem:

$$p(\mathcal{R}_{\rm birth}|1\ \mathrm{obs.}) \propto p(\mathcal{R}_{\rm birth})p(1\ \mathrm{obs.}|\mathcal{R}_{\rm birth}), \quad (7)$$

where $p(\mathcal{R}_{\rm birth})$ is the prior probability on the birthrate of such systems.

If a flat prior is chosen, $p(\mathcal{R}_{\rm birth}) = $ const., the most likely birthrate is $1/t_{\rm W\text{-}R}$, the value used in Equation (2). However, the 90% credible interval on the birthrate extends from $0.35/t_{\rm W\text{-}R}$ (at the 5th percentile) to $4.74/t_{\rm W\text{-}R}$ (at the 95th percentile).

Meanwhile, if an uninformative Jeffreys prior (Jeffreys 1946) on the rate is chosen, $p(\mathcal{R}_{\rm birth}) \propto \mathcal{R}_{\rm birth}^{-1/2}$, the most likely birthrate is halved to $(1/2)/t_{\rm W\text{-}R}$. The 90% credible interval is shifted downward to $0.17/t_{\rm W\text{-}R}$–$3.9/t_{\rm W\text{-}R}$.

Finally, we can consider the case where we assume that there is *at least* one rather than *exactly* one binary in the Galaxy in

[8] https://dcc.ligo.org/cgi-bin/DocDB/ShowDocument?docid=T0900288

[9] In fact, the inspiral–merger–ringdown waveforms we consider here are not accurate for NS systems, but the differences are negligible at low masses.

the same stage as Cyg X-3 (i.e., there may be other similar Galactic systems that have not been observed). In that case, we are interested in $p(\mathcal{R}_{\rm birth}|\geqslant 1$ detection), which scales with $p(\geqslant 1$ detection$|\mathcal{R}_{\rm birth}) = 1-\exp(-\mathcal{R}_{\rm birth} t_{\rm W\text{-}R})$. For the Jeffreys prior, the posterior birthrate distribution peaks at $1.26/t_{\rm W\text{-}R}$.

The merger rate in all cases is given by $\mathcal{R}_{\rm MW} = \mathcal{R}_{\rm birth}/f_{\rm close}$ and so ranges by the same pre-factors relative to the rate given in Equation (2). The large range of purely statistical uncertainty, which spans about a factor of five above and below the value in Equation (2), reflects the difficulty of making robust inference from a single observation.

3. DISCUSSION

We have calculated the future evolution of Galactic binary Cyg X-3 harboring a compact object and a W-R star. We have employed a recent Cyg X-3 component mass estimate from Zdziarski et al. (2012), and following their arguments, we have assumed that the compact object in Cyg X-3 is a black hole.

Our results indicate that the future evolution and fate of Cyg X-3 are a strong function of the mass of the W-R star. Within the measurement uncertainties Cyg X-3 may either form a close BH–BH binary at the high end of the allowed W-R mass ($M_{\rm W\text{-}R} \sim 14\,M_\odot$) or form a close BH–NS (∼15%), a wide BH–NS system (∼15%), or get disrupted producing single BH and NS (∼70%) at the low end and middle of the allowed mass range for the W-R star ($M_{\rm W\text{-}R} \sim 7$–$10\,M_\odot$).

We have estimated the Advanced LIGO/VIRGO detection rates in case of the close BH–BH and BH–NS formation. The rates are significant: in the case of BH–BH formation $\mathcal{R}_{\rm GW} \sim 10\,{\rm yr}^{-1}$. This is the first empirical estimate of a BH–BH detection rate based on a Galactic system. Previous empirical estimates were based on extragalactic high-mass X-ray binaries in the small star-forming galaxies IC 10 and NGC 300 (Bulik et al. 2011). The predicted rates that are based on observations within the Milky Way (high metallicity) are much lower than those estimated for the above two low-metallicity galaxies. The BH–BH detection rate extrapolated from IC 10 X-1 and NGC 300 X-1 for advanced LIGO/Virgo is $\mathcal{R}_{\rm GW} \sim 2000\,{\rm yr}^{-1}$, where we used conservative mass estimates and mean merger rates from Bulik et al. (2011) and converted merger rates to detection rates as discussed in Section 2.3. The low-metallicity environment can significantly boost close BH–BH formation rates. At high metallicity massive star radial expansion occurs primarily during the Hertzsprung gap, while for low-metallicity stars the majority of radial expansion occurs during core-He burning. Massive progenitors of close BH–BH binaries are subject to a common envelope phase. Since Hertzsprung gap stars do not have fully developed core-envelope structure, the CE phase most likely ends in a component merger aborting further binary evolution and preventing the formation of a BH–BH system. This is a major factor in the reduction of the BH–BH merger rate in high-metallicity stellar populations (Belczynski et al. 2007). However, in a low-metallicity environment many close BH–BH systems form via common envelope phase with core He-burning donors (Belczynski et al. 2010b).

The detection rate for BH–NS systems forming via the Cyg X-3 channel is low, $\mathcal{R}_{\rm GW} \sim 0.1\,{\rm yr}^{-1}$. However, our rates are only *lower limits* as more binaries similar to Cyg X-3 may currently exist in the Milky Way and close BH–NS systems may potentially form via other formation channels. Among ∼200 Galactic and extra-galactic high-mass X-ray binaries, only a handful have established parameters (Liu et al. 2005, 2006) allowing for detection rate prediction (Belczynski et al. 2012a). Recent population synthesis calculations provide rates that are typically a few detections per year for BH–NS systems for advanced detectors (Dominik et al. 2012; Belczynski & Dominik 2012). Our prediction is only the second empirical estimate for BH–NS detection rates. The first one was obtained for another Galactic system Cyg X-1 (Belczynski et al. 2011). We note that our current rate (∼1 detection per decade) is 10 times higher than the one obtained for Cyg X-1 (∼1 detection per century).

Beyond our standard evolutionary calculations we have calculated several models to check the validity of our conclusions. We have varied W-R wind mass-loss rates, natal kicks that compact objects receive in supernovae, and the supernova explosion mechanism that alters the NS/BH mass spectrum. Our conclusions are robust, as long as we stay within the framework of the rapid supernova explosion mechanism. We find a range of detection rates $\mathcal{R}_{\rm GW} = 0.09$–$0.15\,{\rm yr}^{-1}$ for BH–NS systems and $\mathcal{R}_{\rm GW} = 7.7$–$12.4\,{\rm yr}^{-1}$ for BH–BH systems. Our standard supernova model, which employs rapid explosions, is motivated by the existence of the mass gap between NSs and BHs (e.g., Bailyn et al. 1998; Özel et al. 2010; Farr et al. 2011). However, if the mass gap is not an intrinsic signature of the BH/NS mass spectrum but is caused by some observational bias as recently claimed by Kreidberg et al. (2012), our conclusions change. For the delayed supernova model, which is consistent with the absence of a mass gap, we find that BH–NS formation occurs only at the lowest allowed mass for the W-R star in Cyg X-3 ($M_{\rm W\text{-}R} \sim 7\,M_\odot$) with a slightly higher detection rate $\mathcal{R}_{\rm GW} = 0.17\,{\rm yr}^{-1}$. BH–BH formation is found in a broader mass range allowed for the W-R star ($M_{\rm W\text{-}R} \sim 10$–$14\,M_\odot$). The second BH falls right within the mass gap ($M_{\rm BH2} = 2.7$–$3.9\,M_\odot$), and the rates are significantly smaller, $\mathcal{R}_{\rm GW} = 0.41$–$2.8\,{\rm yr}^{-1}$. Finally, we note that all merger and detection rates have statistical uncertainties of approximately a factor of five in either direction due to the limited observational sample of a single system.

Authors acknowledge support from MSHE grant N203 404939, N203 511238 (K.B.) and NASA Grant NNX09AV06A to the UTB Center for Gravitational Wave Astronomy (K.B.). A.A.Z. acknowledges support from the Polish NCN grant Nos. N203 581240 and 2012/04/M/ST9/00780, and T.B., support from 623/N-VIRGO/09/2010/0. K.B., I.M., and B.S. acknowledge the hospitality of KITP, supported in part by the National Science Foundation under NSF Grant PHY11-25915. B.S. was supported by the Science and Technology Facilities Council (STFC), UK Grant No. ST/J000345/1.

REFERENCES

Abadie, J., Abbott, B. P., Abbott, R., et al. 2010, CQGra, 27, 173001
Acernese, F., Amico, P., Alshourbagy, M., et al. 2006, CQGra, 23, S635
Ajith, P., Hannam, M., Husa, S., et al. 2011, PhRL, 106, 241101
Bailyn, C., Jain, R., Coppi, P., & Orosz, J. 1998, ApJ, 499, 367
Belczynski, K., Bulik, T., & Bailyn, C. 2011, ApJL, 742, L2
Belczynski, K., Bulik, T., & Fryer, C. 2012a, ApJ, in press (arXiv:1208.2422)
Belczynski, K., Bulik, T., Fryer, C., et al. 2010a, ApJ, 714, 1217
Belczynski, K., & Dominik, M. 2012, ApJ, submitted (arXiv:1208.0358)
Belczynski, K., Dominik, M., Bulik, T., et al. 2010b, ApJL, 715, L138
Belczynski, K., Taam, R., Kalogera, V., Rasio, F., & Bulik, T. 2007, ApJ, 662, 504
Belczynski, K., Wiktorowicz, G., Fryer, C., Holz, D., & Kalogera, V. 2012b, ApJ, 757, 91
Bulik, T., Belczynski, K., & Prestwich, A. 2011, ApJ, 730, 140
Claret, A. 2007, A&A, 467, 1389
Dominik, M., Belczynski, K., Fryer, C., et al. 2012, ApJ, 759, 52

Ergma, E., & Yungelson, L. R. 1998, A&A, 333, 151
Farr, W., Sravan, N., Cantrell, A., et al. 2011, ApJ, 741, 103
Finn, L. S. 1996, PhRD, 53, 2878
Fryer, C., Belczynski, K., Wiktorowicz, G., et al. 2012, ApJ, 749, 91
Georgy, C., Ekström, S., Meynet, G., et al. 2012, A&A, 542, 29
Hamann, W., & Koesterke, L. 1998, A&A, 335, 1003
Harry, G. M. (for the LIGO Scientific Collaboration) 2010, CQGra, 27, 084006
Hobbs, G., Lorimer, D., Lyne, A., & Kramer, M. 2005, MNRAS, 360, 974
Hogg, D. W. 1999, arXiv:astro-ph/9905116
Hurley, J., Pols, O., & Tout, C. 2000, MNRAS, 315, 543
Jeffreys, H. 1946, RSPSA, 186, 453
Kreidberg, L., Bailyn, C., Farr, W., & Kalogera, V. 2012, ApJ, 757, 36
Liu, Q. Z., van Paradijs, J., & van den Heuvel, E. P. J. 2005, A&A, 442, 1135
Liu, Q. Z., van Paradijs, J., & van den Heuvel, E. P. J. 2006, A&A, 455, 1165
Lommen, D., Yungelson, L., van den Heuvel, E., Nelemans, G., & Portegies Zwart, S. 2005, A&A, 443, 231
Lorimer, D. 2008, LRR, 11, 8
Nugis, T., & Lamers, H. 2000, A&A, 360, 227
Özel, F., Psaltis, D., Narayan, R., & McClintock, J. E. 2010, ApJ, 725, 1918
Podsiadlowski, Ph., Langer, N., Poelarends, A., et al. 2004, ApJ, 612, 1044
Weisberg, J. M., & Taylor, J. H. 2005, in ASP Conf. Ser. 328 Binary Radio Pulsars, ed. F. A. Rasio & I. H. Stairs (San Francisco, CA: ASP), 25
Zdziarski, A. A., Mikołajewska, J., & Belczynski, K. 2012, MNRAS, in press (arXiv:1208.5455)